J. Biochem. **134**, 881–891 (2003)
DOI: 10.1093/jb/mvg215

Effects of Essential Carbohydrate/Aromatic Stacking Interaction with Tyr100 and Phe259 on Substrate Binding of Cyclodextrin Glycosyltransferase from Alkalophilic *Bacillus* sp. 1011

Keiko Haga[*,1], Ryuta Kanai[*,1,2], Osamu Sakamoto[1], Masanobu Aoyagi[1], Kazuaki Harata[†,2] and Kunio Yamane[‡,1]

[1]Institute of Biological Sciences, University of Tsukuba, Tsukuba, Ibaraki 305-8572; and [2]Biological Information Research Center, National Institute of Advanced Industrial Science and Technology, Tsukuba, Ibaraki 305-8566

Received July 25, 2003; accepted October 7, 2003

The stacking interaction between a tyrosine residue and the sugar ring at the catalytic subsite –1 is strictly conserved in the glycoside hydrolase family 13 enzymes. Replacing Tyr100 with leucine in cyclodextrin glycosyltransferase (CGTase) from *Bacillus* sp. 1011 to prevent stacking significantly decreased all CGTase activities. The adjacent stacking interaction with both Phe183 and Phe259 onto the sugar ring at subsite +2 is essentially conserved among CGTases. F183L/F259L mutant CGTase affects donor substrate binding and/or acceptor binding during transglycosylation [Nakamura *et al.* (1994) *Biochemistry* 33, 9929–9936]. To elucidate the precise role of carbohydrate/aromatic stacking interaction at subsites –1 and +2 on the substrate binding of CGTases, we analyzed the X-ray structures of wild-type (2.0 Å resolution), and Y100L (2.2 Å resolution) and F183L/F259L mutant (1.9 Å resolution) CGTases complexed with the inhibitor, acarbose. The refined structures revealed that acarbose molecules bound to the Y100L mutant moved from the active center toward the side chain of Tyr195, and the hydrogen bonding and hydrophobic interaction between acarbose and subsites significantly diminished. The position of pseudo-tetrasaccharide binding in the F183L/F259L mutant was closer to the non-reducing end, and the torsion angles of glycosidic linkages at subsites –1 to +1 on molecule 1 and subsites –2 to –1 on molecule 2 significantly changed compared with that of each molecule of wild-type-acarbose complex to adopt the structural change of subsite +2. These structural and biochemical data suggest that substrate binding in the active site of CGTase is critically affected by the carbohydrate/aromatic stacking interaction with Tyr100 at the catalytic subsite –1 and that this effect is likely a result of cooperation between Tyr100 and Phe259 through stacking interaction with substrate at subsite +2.

Key words: acarbose, alkalophilic *Bacillus* sp. 1011, cyclodextrin glycosyltransferase, stacking interaction, X-ray crystal structure.

Abbreviations: α-CHA, α-cyano-4-hydroxycinnamic acid; CGTase, cyclodextrin glycosyltransferase; G1-CNP, 2-chloro-4-nitrophenyl β-glucoside; G2-CNP, 2-chloro-4-nitrophenyl β-maltoside; G3-CNP, 2-chloro-4-nitrophenyl β-maltotrioside; G4-CNP, 2-chloro-4-nitrophenyl β-maltotetraoside; GlcAcvGlc, α-D-glucopyranosyl-α-acarviosinyl-D-glucopyranose; 3KB-G5-CNP, 3-ketobutylidene-2-chloro-4-nitrophenyl β-maltopentaoside; MALDI-TOF/MS, Matrix-Assisted Laser Desorption Ionization Time-Of-Flight Mass Spectrometry; PTS, pseudotrisaccharide or acarviosine-glucose; Sfamy, *Saccharomycopsis fibuligera* α-amylase.

Cyclodextrin glycosyltransferase (CGTase) [EC 2.4.1.19] catalyzes the conversions of starch and amylose into a mixture of α-, β-, and γ-cyclodextrins (CD) that consist of six, seven and eight D-glucose residues, respectively. Besides this cyclization, the enzyme also catalyzes coupling (the reverse of cyclization), disproportionation (intermolecular transglycosylation) and weak hydrolysis. Cyclodextrins form inclusion complexes with various molecules and alter the chemical and physical properties of the included molecules. Therefore, CGTases are important enzymes with wide industrial applications. Structural studies and protein engineering approaches have revealed that CGTase is a member of the α-amylase family (glycoside hydrolase family 13) with four highly conserved regions designated I, II, III and IV (*1–3*), and catalytic domains that are folded into $(\beta/\alpha)_8$-barrel structures (*4–9*). Variations in substrate specificity and reaction products of glycoside hydrolase family 13 enzymes are associated with the fact that although their catalytic centers are similar, their subsite structures differ (*10*).

To define the functional differences between CGTases and α-amylases, we have examined the structure/function relationships of CGTase from the alkalophilic bacterium *Bacillus* sp. 1011 (*10–13*) using protein engineering approaches. The enzyme that predominantly produces β-CD has high starch-degrading activity over a wide pH range (4.5–10.5) at 37°C. We crystallized the CGTase and

[*]These authors contributed equally to this work.
[†]Atomic coordinates for the complex have been deposited with the Brookhaven Protein Data Bank (file names: wild-type-acarbose, 1UKQ; F183L/F259L-acarbose, 1UKS; Y100L-acarbose, 1UKT).
[‡]To whom correspondence should be addressed. Tel & Fax: +81-29-853-6680, E-mail address: kyamane@sakura.cc.tsukuba.ac.jp

Table 1. **Partially aligned amino acid sequences in the active sites of family 13 Enzymes.**

Enzymes	Accession number/Reference	Sequence
Cyclodextrin glycosyltransferase		
alkalophilic *Bacillus* sp. 1011	P05618	90 SGVNNTAYHG**Y**WARDFKKTNP
Bacillus circulans strain 251	P43379	90 SGVNNTAYHG**Y**WARDFKKTNP
Bacillus licheniformis	P14014	90 SGVTNTAYHG**Y**WARDFKKTNP
Thermoanaerobacterium thermosulfurigenes EM1	P26827	93 GG--STSYHG**Y**WARDFKRTNP
alkalophilic *Bacillus* sp. 38-2	P09121	90 SGVHNTAYHG**Y**WARDFKKTNP
Bacillus ohbensis	P27036	92 -----TSYHG**Y**WARDYKRTNP
*Bacillus circulans*strain 8	P30920	97 SGVTNTAYHG**Y**WARDFKKTNP
Bacillus stearothermophilus	P31797	88 SGS--ASYHG**Y**WARDFKKPNP
Bacillus macerans	P04830	90 SGVNNTSYHG**Y**WARDFKQTND
α-amylase		
Bacillus subtilis	P00691	54 SMSN--WYWL**Y**-QPTSYQIGN
Aspergillus oryzae	P10529	75 YGD---AYTG**Y**WQTDIYSLNE
Saccharomycopsis fibuligera	P21567	76 YGY---AYHG**Y**WMKNIYKINE
Porcine pancreatic	P00690	55 SR---PWWER**Y**-QPVSYKLCT
Barley	Rogers *et al*. 1983 (*46*)	70 SVSN----EG**Y**MPGRLYDIDA
Neopullulanase		
Bacillus stearothermophilus	P38940	206---------K**Y**DTADYFEVDP
α-glucosidase		
Bacillus sp. SAM1606	Nakao *et al*. 1994 (*47*)	72 SPND---DMG**Y**DIRDYYKIME
oligo-1,6-glucosidase		
Bacillus thermoglucosidasius	P29094	56 SPND---DNG**Y**DISDYRDIMD

Gaps are denoted by –.

determined its three-dimensional structure at 1.8 Å resolution (*14*, *15*). The unit cell contained two independent molecules related through a pseudo-twofold symmetry. This enzyme consists of domains, A, B, C, D, and E, and its backbone structure is similar to that of four other homologous CGTases (*8*, *9*, *16*, *17*).

Crystallographic studies of ligand-complexed CGTase from *Bacillus circulans* strain 251 (*18–21*) and *B. circulans* strain 8 (*22*, *23*) revealed substrate-recognition sites designated from +2 to –7 for binding oligosaccharides, and subsites –4c, +4c and +3c for CD binding with a catalytic site between subsites –1 and +1. The structure of the CGTase complex with the covalently bound reaction intermediate indicates that Tyr100 (stacking interaction) together with Trp75 and Arg227 tightens the hydrogen bond interaction network (*20*). When a linear substrate binds to the active site of CGTase, stacking interactions between substrate and Phe183 and Phe259 occur at subsite +2 (*18*). During CD binding, the aromatic side chain of Phe259 stacks only onto the glucosyl unit at subsite +2 (*19*).

Tyr100 together with other residues of the subsite –1 architecture is highly conserved in the glycoside hydrolase family 13 (Table 1) and seems to play a crucial role in the substrate binding of glycoside hydrolase family 13 enzymes (*20*). However, replacing Tyr83 (equivalent to Tyr100) on *Saccharomycopsis fibuligera* α-amylase (Sfamy) with tryptophan, leucine or aspartic acid, significantly enhanced transglycosylation activity and produced a complementary decrease in native hydrolysis activity (*24*). To determine the roles of carbohydrate/aromatic stacking interaction with Tyr100 at subsite –1 of CGTase, we replaced Tyr100 with leucine and phenylalanine using site-directed mutagenesis and characterized purified mutants with respect to substrate binding and activity of CGTase.

Sequence comparisons among CGTases and α-amylases have revealed that Phe183 and Phe259 are highly conserved among CGTases but are replaced with aliphatic or aromatic residues in α-amylases. The amino acid residue in the position equivalent to Phe259 of α-amylases is mostly an aliphatic residue, and that equivalent to Phe183 is tyrosine, tryptophan, proline, glutamine or others. Therefore, the stacking interaction of both Phe183 and Phe259 with bound sugar residues found among CGTases does not arise in α-amylases. We proposed that the F183L/F259L mutation in CGTase affects donor substrate and/or acceptor binding during transglycosylation (*13*). To investigate the effects of Leu100 and both Leu183 and Leu259 on substrate binding of the catalytic site of CGTase in the absence of stacking, we analyzed the structures of wild-type (2.0 Å resolution), and Y100L (2.2 Å resolution) and F183L/F259L (1.9 Å resolution) mutant CGTases complexed with the inhibitor, acarbose.

We describe the critical importance of Tyr100 for CGTase to bind substrate CGTase and the features that differ between Y100L (CGTase) and Y83L (Sfamy) mutants due to specific stacking interaction with Phe183 and/or Phe259. Furthermore, we discuss the contribution of the carbohydrate/aromatic stacking interaction of Tyr100 and Phe259 to the substrate binding in the active site of CGTase.

MATERIALS AND METHODS

Chemicals and Enzymes—All restriction and modification enzymes used for recombinant DNA manipulations were purchased from Takara Shuzo or Toyobo. Tetracy-

Table 2. **Statistics of data collection (A) and structure refinement (B).**

	Wild-type Acarbose	F183L/F259L-Acarbose	Y100L-Acarbose
(A) Data collection			
Space group	*P*1	*P*1	*P*1
Cell dimension			
a (Å)	64.95	64.85	65.68
b (Å)	74.49	74.53	74.47
c (Å)	79.10	85.19	80.10
α (deg)	85.13	85.19	85.29
β (deg)	105.02	104.19	105.59
γ (deg)	101.02	101.04	100.81
Resolution range	48.55–2.00	19.80–1.91	76.77–2.01
No. unique reflections	91,157	102,881	68,926
R_{merge}	0.132	0.048	0.068
(B) Structure refinement			
No. of atoms			
Protein	10,624	10,612	10,618
Calcium	4	4	4
Acarbose	88	88	88
Solvent water	638	739	253
Resolution range	10.0–2.0	10.0–1.9	10.0–2.2
No. of reflections	82,018 (>1σ)	85,845 (>2σ)	40,829 (>2σ)
R-value	0.184	0.162	0.173
R_{free}	0.246	0.215	0.276
RMSD bond (Å)	0.013	0.014	0.009
RMSD angle (deg)	3.01	2.79	1.52

cline and ampicillin were from Wako Pure Chemical Industry. Soluble starch was from Merck (Art. 1252). Amylose (average degree of polymerization, 17) was a gift from Hayashibara Biochemical Laboratories. Acarbose (Bay-g-5421) was a gift from Drs. A. Mullen and K. Hornberg (Bayer AG). 3KB-G5-CNP (3-ketobutylidene-2-chloro-4-nitrophenyl β-maltopentaoside) and CNP-maltooligosaccharide standards were purchased from Toyobo. All other chemicals were of reagent grade.

Bacterial Strains and Plasmids—Recombinant DNA was manipulated in *Escherichia coli* JM109 [*recA1 endA1 gyrA96 thi hsdR17 supE44 relA1Δ* (*lac proAB*)/F′: *traD36 proAB lacI*^{q} *ZΔM15*]. Wild-type and mutant CGTases were produced in the protease-deficient mutant, *E. coli* ME8417 [*lon*::Tn*10*(*tet*^{r}) *thr leu lacY*], provided by Dr. H. Takahashi (The University of Tokyo). Plasmid pTUE254 was constructed by inserting the 4.5 kb *Hin*dIII fragment of pTUE217 (*2*), which contains the CGTase gene region of the alkalophilic *Bacillus* sp. 1011, into the *Hin*dIII site of pUC13.

Mutant CGTase Genes—Mutant CGTase genes encoding either the Y100L or the Y100F mutant were obtained by the site-directed mutagenesis of pTUE254 according to Kunkel (*25*) with slight modifications as described (*13*). The mutations were verified by DNA sequencing (*26*). The following oligonucleotides were used to create the mutations (underline denotes mutations and codons, respectively):

Y100F mutant: 5′-TCACGGCTTCTGGGCCC-3′

Y100L mutant: 5′-CTTATCACGGCTTGTGGGCCCGG-3′

Clones expressing CGTase activity were scored on plates containing Luria-Bertani medium agar with 1% soluble starch.

Expression and Purification of Wild-type, Y100L- and Y100F-CGTases—*Escherichia coli* ME8417 transformants carrying constructs were cultured in 1 liter of Luria-Bertani medium [1% bacto-tryptone (Difco), 0.5% yeast extract (Difco), and 0.5% sodium chloride], containing 250 μg/ml ampicillin and 20 μg/ml tetracycline at 37°C for 12 h. Wild-type and mutant CGTases in the periplasm of the cells were extracted by osmotic shock (*27*) and purified as described (*10*). F183L, F259L, and F183L/F259L mutant CGTases were purified as described (*13*).

Enzyme Assay—All reactions proceeded at 37°C in 10 mM sodium phosphate buffer at pH 6.5. Starch-degrading activity and disproportionation activity between 3KB-G5-CNP and maltose were determined as described (*10*, *12*). The acarbose concentrations required for 50% inhibition of the starch-degrading activity (IC_{50}) were measured using the blue value method of Fuwa as described (*11*).

Bond-cleavage Profiles of 3KB-G5-CNP—Bond-cleavage profiles were determined using a slight modification of the transglycosylation assay as follows. Reaction mixtures containing 1–100 nM enzyme, 1 mM 3KB-G5-CNP as a donor substrate and 50 mM glucose as an acceptor were incubated at 37°C for 5–15 min. Primary products prior to 15% conversion were identified at appropriate intervals thereafter. The reaction was stopped by adding 20 μl of 0.2 N hydrochloric acid to 200 μl of the mixture, and then 20 μl of 0.5 M disodium hydrogen phosphate was added. The reaction products were quantified at 20°C by HPLC on a LiChrosorb NH_2 column (mean particle size, 5 μm; 4 × 250 mm; Cica-Merck) and monitored using an ultraviolet detector (Beckman System Gold) at 313 nm. The mobile phase was 80% acetonitrile at a flow rate of 0.8 ml/min. Separated reaction products were

Table 3. **Binding modes and torsion angles for acarbose and related compounds bound to wild-type and mutant CGTases.**

		(A) Binding modes subsites					
Enzyme complex		–4	–3	–2	–1	+1	+2
Wild-type	Molecule 1			G	C	DG	G
	Molecule 2			G	C	DG	G
F183L/F259L	Molecule 1		G	C	DG	G	
	Molecule 2	G	C	DG	G		
Y100L	Molecule 1			C	DG	G	G
	Molecule 2		C	DG	G	G	

		(B) Torsion angles[a]									
		sites –4/–3		sites –3/–2		sites –2/–1		sites –1/+1		sites +1/+2	
Enzyme complex		ϕ	ψ	ϕ	ψ	ϕ	ψ	ϕ	ψ	ϕ	ψ
Wild-type	Molecule 1					149.04	–98.61	57.68	–105.02	51.27	–150.97
	Molecule 2					117.08	–98.19	43.61	–103.40	85.38	–158.44
F183L/F259L	Molecule 1			137.83	–90.41	98.05	–105.15	59.30	–153.08		
	Molecule 2	159.03	–90.88	122.63	–162.14	76.24	–132.86				
Y100L	Molecule 1					30.24	–164.49	40.35	44.67	139.35	76.20
	Molecule 2			147.35	–87.15	111.26	–113.10	150.70	–65.39		

Abbreviations: G, α-D-glucose; C, cyclitol of acarbose; DG, 4-amino-4, -α-D-dideoxyglucose of acarbose. [a]ϕ = torsion angle O5(C7)-C1-O4′(N4′)-C4′. ψ=torsion angle C1-O4′(N4′)-C4′-C5′. Torsion angles for subsites –4 to +2 are given.

identified and calibrated by comparison with 1% G1-CNP, G2-CNP, G3-CNP, and G4-CNP standards.

Thin-Layer Chromatography (TLC)—Reaction mixtures were analyzed by TLC using Kieselgel 60F 254 plates (Merck) and a solvent system of ethyl acetate/isopropyl alcohol/water (1:3:1, v/v/v). After being developed twice, the TLC plates were dried and visualized by spraying with 0.3% (w/v) *N*-(1-naphthyl)-ethylenediamine and 5% (v/v) H_2SO_4 in methanol and heating at 120°C for 15 min. To prepare each reaction product, we incubated 10 mM acarbose solution (1 ml) with 20 mg of wild-type, F183L/F259L, and Y100L mutant CGTases (1 ml) at 37°C for 2 weeks. The reaction mixture separated by TLC was visualized, then each reaction product was extracted with Milli-Q water for 1 h and lyophilized.

Matrix-Assisted Laser Desorption Ionization Time-of-Flight Mass Spectrometry (MALDI-TOF/MS) Analysis—The MALDI-TOF/MS spectra were collected using a Voyager-DE (Applied Biosystems), and α-cyano-4-hydroxycinnamic acid (α-CHCA) was used as a matrix. One microliter of the purified sample and α-CHCA was dropped on a sample plate and thoroughly dried. The sample plate was placed in the Voyager-DE Biospectrometry workstation operated at an acceleration voltage of 20 kV.

Co-crystallization and Data Collection—Crystals of wild-type and mutant CGTases complexed with acarbose were obtained by co-crystallization for 1–2 weeks in 0.1 M sodium citrate buffer, pH 5.6 containing 1% protein, 1 mM acarbose, 20% (w/v) polyethylene glycol 3000, 20% (v/v) 2-propanol and 0.5 mM $CaCl_2$ at room temperature. Crystals of inhibitor complexes were isomorphous with those of native CGTase. The space group *P*1 was same as that of the native CGTase (*14*), and the unit cell of each complex contained two independent molecules (V_m = 2.41 Å^3 Da^{-1}). X-ray diffraction data of the wild-type-acarbose complex were collected to 2.0 Å resolution on a Bruker SMART 6000 diffractometer (50 kV, 90 mA, focal spot size 0.3 mm). X-ray diffraction data from F183L/F259L complexed with acarbose were collected at 1.9 Å resolution on an Enraf-Nonius FAST diffractometer (40 kV, 45 mA focal spot size 0.2 mm). X-ray diffraction data from Y100L mutant complexed with acarbose were collected at 2.2 Å resolution on a Rigaku R-AXIS IIC diffractometer (40 kV, 50 mA). Data collection statistics are summarized in Table 2.

Structure Determination and Refinement—Structures were determined by the molecular-replacement method using the 1.8 Å structure of wild-type CGTase (*15*) consisting of two independent CGTases and four calcium ions as the starting model. The crystal structures were refined with the program *X-PLOR* (*29*), based upon reflections in the resolution range 10–2.0 Å (>1σ), 10–1.9 Å (>2σ), and 10–2.2 Å (>2σ), for wild-type, F183L/F259L and Y100L mutant CGTases, respectively. Acarbose molecules were identified on $|3F_0 - 2F_c|$ and $|F_0 - F_c|$ electron density maps (>1.5σ) in the catalytic active site. All stereo figures were produced using the program TURBO-FRODO. Refinement statistics are listed in Table 2. The qualities of the final models were checked using the program PROCHECK (*30*). Atomic coordinates have been deposited with the Protein Data Bank (entry code: wild-type-acarbose, 1UKQ; F183L/F259L-acarbose, 1UKS; Y100L-acarbose, 1UKT).

RESULTS

Structure Determination—We determined the crystal structure of each CGTase-acarbose complex to compare the modes of the acarbose binding. Table 2 summarizes the crystallographic results. The structures of the acarbose complexes of wild-type, F183L/F259L, and Y100L mutants were determined by the molecular-replacement method using the native structure of wild-type CGTase at 1.8 Å (*15*). Crystal structures were refined to *R* values of 0.184, 0.162, and 0.173 with free *R* values of 0.246, 0.215, and 0.276 for wild-type and F183L/F259L and Y100L mutants, respectively. These crystals were nearly isomorphous with the native crystals and the asymmetric unit contained two CGTase molecules, two acarbose molecules and four calcium ions. The backbone structure of each complex was essentially identical to the structure of native CGTase (*15*), and was very similar to that of other

Table 4. **Starch-degrading and disproportionation activities of wild-type and mutant CGTases[a].**

Enzymes	Starch-degrading Activity (units/mg)	Disproportionation Activity			
		3KB-G5-CNP k_{cat} (s^{-1})	3KB-G5-CNP K_m (mM)	Maltose K_m (mM)	3KB-G5-CNP k_{cat}/K_m (s^{-1} mM^{-1})
Wild-type	2,170[b]	203 ± 3[b]	0.16 ± 0.01[b]	0.49 ± 0.02[b]	1,269
F183L	338[b]	333 ± 8[b]	0.08 ± 0.01[b]	1.42 ± 0.09[b]	4,111
F259L	869[b]	25.4 ± 0.8[b]	0.48 ± 0.01[b]	1.30 ± 0.08[b]	52
F183L/F259L	79.0[b]	158.4 ± 4[b]	0.24 ± 0.02[b]	18.22 ± 0.4[b]	660
Y100F	1,430	14.2 ± 1.8	0.14 ± 0.06	0.05 ± 0.02	101
Y100L	0.4	N.D.	N.D.	N.D.	N.D.

[a]Assays were performed in 10 mM sodium phosphate, pH 6.5 at 37°C. [b]Data already reported (*13*). N.D.: not determined.

CGTases (*8*, *9*, *16*, *17*). All amino acid residues in direct contact with acarbose were well defined in the electron density maps. The largest changes in the protein backbone structure were in the order of 3 Å. The omit $|F_o - F_c|$ electron density maps of acarbose on wild-type, F183L/F259L and Y100L mutants are shown in Figs. 3, 4, and 5 respectively, and the manner of acarbose binding to each CGTase is shown in Table 3A.

Characterization of F183L/F259L and Y100L Mutants—Our previous results (*13*) and Table 4 indicated that the F183L mutantion more specifically affects the binding of the acceptor than of the donor in the disproportionation reaction. This is because the K_m value of this mutant for acceptor maltose increased 3-fold, whereas that for donor 3KB-G5-CNP was one half that of the wild-type. On the other hand, the F259L mutantation affects the binding of both the donor and the acceptor, since the K_m value for donor 3KB-G5-CNP increased 3-fold and the k_{cat} corresponded to 12% of the wild-type value. In the double mutant F183L/F259L, the K_m for donor 3KB-G5-CNP was intermediate between those of the F183L and F259L mutants. The IC_{50} values of acarbose for F183L and F259L mutants were 64- and 70-fold higher than that of wild-type, respectively. In contrast, the IC_{50} values for the F183L/F259L mutant increased 10,000-fold (Table 5).

Characterization of the purified Y100L and Y100F mutants allowed a detailed comparison of their properties with those of wild-type, F183L, F259L, and F183L/F259L mutants (Table 4). To remove the stacking interaction with the sugar ring while retaining hydrophobicity at subsite –1, we replaced phenylalanine with leucine, which has a short aliphatic side chain. Alternatively, phenylalanine was introduced to retain the aromatic side chain and the stacking interaction with substrate. Starch-degrading activity and cyclization efficiency of the Y100L mutant were reduced to 0.02% and 0.01% (not shown) of the wild-type value, respectively, and disproportionation activity was undetectable. On the other hand, the amount of starch-degrading activity and the k_{cat} for the disproportionation reaction of the Y100F mutant were reduced to 66% and 7% of the wild-type value, respectively. Although the K_m for the donor (3KB-G5-CNP) of the Y100F mutant did not significantly change, that for the acceptor (maltose) decreased 10-fold compared with the wild-type. Despite the retention of the carbohydrate/aromatic stacking interaction at subsite –1, the mutation of Tyr100 to phenylalanine significantly affected CGTase activities. These characteristic differences affected the IC_{50} values of acarbose for starch-degrading activity (Table 5). The IC_{50} value for the Y100F mutant was 109-fold higher than that of the wild-type, but the value for the Y100L mutant increased over 17,000-fold. Such a high IC_{50} value has not been found in other alkalophilic *Bacillus* sp. 1011 CGTase mutants analyzed to date (*11*, *13*).

Identification of the Bound Pseudo-tetrasaccharide in Each Acarbose-Enzyme Complex—Acarbose is a pseudo-tetrasaccharide with two glucosyl groups attached to the reducing end of the acarviosine moiety, which is composed of cyclitol and 4-amino-4, 6-dideoxy-D-glucose (6-deoxyglucose) (Fig. 1A). The three-dimensional structures of other enzymes of the α-amylase family except for amylomaltase from *Thermus aquaticus* (*31*) revealed that acarbose is processed and that the inhibitory cyclitol ring of acarbose, which mimics the half chair conformation of the transition state, binds to catalytic subsite–1 (*32*–*36*).

We examined the pseudo-tetrasaccharide bound to each CGTase-acarbose complex as follows. We analyzed the reaction products of acarbose with wild-type, F183L/F259L and Y100L mutant CGTases by TLC and by MALDI-TOF/MS (see "MATERIALS AND METHODS") according to the analytical method for α-D-glucopyranosyl-α-acarviosinyl-D-glucopyranose (GlcAcvGlc) (Fig. 1B) from the hydrolysate of a high-molecular-weight acarbose by *Thermus* maltogenic amylase (ThMA) (*37*).

Only three products (spots 1, 2, and 3) were apparent from the reaction of acarbose with wild-type and F183L/F259L mutant CGTases, whereas no products were generated from the reaction of acarbose with the Y100L mutant CGTase (Fig. 2A). When spot 3 was incubated with glucoamylase from *Aspergillus niger*, the reaction gave spots 1 and 2 (Fig. 2B). In addition, MALDI-TOF/MS data (not shown) for each spot suggested that spots 1, 2, and 3 corresponded to D-glucose (M), acarviosine-D-glucose (pseudo-trisaccharide) (PTS) (M) and GlcAcvGlc

Table 5. **Acarbose concentrations required for 50% inhibition of the starch-degrading activity (IC_{50})[a].**

Enzymes	IC_{50} (10^{-6}M)	Ratio
Wild-type	0.33[b]	1
F183L/F259L	3,300	10,000
F183L	21[b]	64
F259L	23[b]	70
Y100F	36	109
Y100L	≫5,600	≫17,000

[a]Assays were performed in 10 mM sodium phosphate, pH 6.5 at 37°C. [b]Data already reported (*13*).

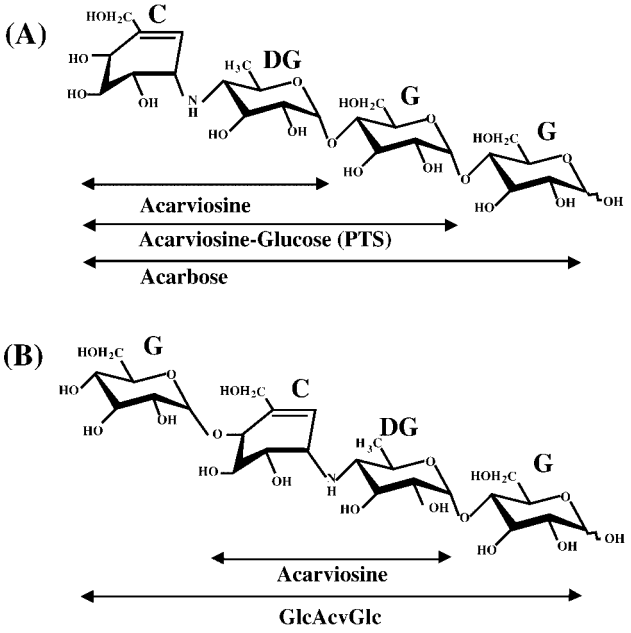

Fig. 1. **Initial and processed acarbose structures.** (A) Structure of acarbose. Acarviosine moiety is composed of cyclitol (hydroxymethylconduritol unit) and 4-amino-4,6-dideoxy-D-glucose. PTS is composed of acarviosine and D-glucose. From the non-reducing end of acarbose, cyclitol unit is labeled C, 4-amino-4, 6-dideoxy-D-glucose is labeled DG and D-glucose is labeled G. (B) Structure of processing product of acarbose (GlcAcvGlc).

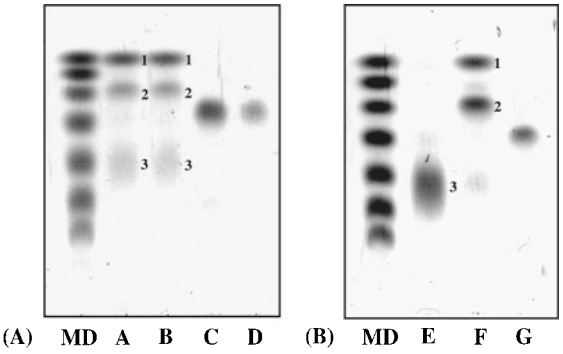

Fig. 2. **TLC analysis of reaction products.** (A) TLC of acarbose digested with wild-type, F183L/F259L and Y100L mutant enzymes for 2 weeks at 37°C. (B) TLC of spot 3 digested with glucoamylase from *Aspergillus niger* for 24 h at 37°C. MD, maltodextrin standards (G1–G7). Lane A, reaction products of acarbose with the wild-type enzyme; lane B, reaction products of acarbose with the F183L/F259L mutant; lane C, reaction products of acarbose with the Y100L mutant; lanes D and G, acarbose; lane E, intact spot 3; lane F, reaction products of spot 3 with glucoamylase. Spot 1, glucose; spot 2, pseudotrisaccharide (PTS); spot 3, pseudotetrasaccharide (GlcAcvGlc). MD and spot 1 showed black. Spots for acarbose, 2 and 3 showed dark purple.

(M) (Fig. 1), because each spectrum at mass (m/z) values of 181.37, 484.20, and 646.22 represented combination with a proton [$(M+H)^+$], respectively. We therefore suggest that each pseudo-tetrasaccharide bound to wild-type and F183L/F259L mutant CGTases is likely to be GlcAcvGlc and that acarbose binds to the Y100L mutant.

Structural Characteristics of Pseudo-tetrasaccharide Bound in the Active Site of Wild-type, F183L/F259L and Y100L CGTases—The electron density map of the occupied subsites –2 to +2 showed GlcAcvGlc in the active site of each molecule of wild-type CGTase (Fig. 3). The carbohydrate/aromatic stacking interaction was found in the active site of GlcAcvGlc-binding wild-type CGTase, in which the side chain group of Tyr100 at subsite –1 was approximately parallel to the plane of the cyclitol ring of GlcAcvGlc. The phenyl ring of Phe259 of molecule 1 stacked the D-glucose at subsite +2 (Fig. 3A), and the phenyl rings of both Phe183 and Phe259 at subsite +2 of molecule 2 sandwiched the D-glucose residue (Fig. 3B). Therefore, the interaction between each sugar ring of GlcAcvGlc and each aromatic ring of Phe183 and Phe259 at subsites +1 to +2 on molecule 1 are almost identical to those between the corresponding sugar ring of γ-CD and the aromatic rings of Phe183 and Phe259 in the γ-CD complex (*19*) (Fig. 6A), in contrast, those on molecule 2 are also similar to the equivalent ones of the maltononaose complex (*18*) (Fig. 6B).

The binding modes of GlcAcvGlc in the two independent molecules of the F183L/F259L mutant differed from that in the wild-type (Fig. 4 and Table 3A). That is, GlcAcvGlc bound to molecule 1 occupied subsites –3, –2, –1, and +1, while on molecule 2 it considerably shifted towards subsite –4 (occupying subsites –4, –3, –2, and –1). As a result, polar contacts between the sugar residues of GlcAcvGlc and amino acid residues in the F183L/F259L mutant significantly changed and decreased in number (not shown). The catalytic residues Asp229 and Glu257 of F183L/F259L mutant form hydrogen bonds with 4-amino-4, 6-dideoxy-D-glucose and D-glucose resi-

Table 6. **Bond-cleavage profiles in the disproportionation reaction of 3KB-G5-CNP by wild-type and mutant CGTases.**

Bond[a]		1		2		3		4		5	
Wild-type	3KB-G	–	G	–	G	–	G	–	G	–	CNP
		0		0		0.59		0.41		0	
F183L	3KB-G	–	G	–	G	–	G	–	G	–	CNP
		0		0		0.09		0.91		0	
F259L	3KB-G	–	G	–	G	–	G	–	G	–	CNP
		0		0		0.66		0.34		0	
F183L/F259L	3KB-G	–	G	–	G	–	G	–	G	–	CNP
		0		0		0		1.0		0	

Abbreviations: G, α-D-glucose; 3KB-G5-CNP, 3-ketobutylidene-2-chloro-4-nitrophenyl β-maltopentaoside [a]Bonds 1, 2, 3, and 4 are α-1,4-glycosidic bonds, and bond 5 is a β-glycosidic bond between glucose and 1-chloro-4-nitrophenol. The numbers indicated are normalized frequencies at each cleavage position.

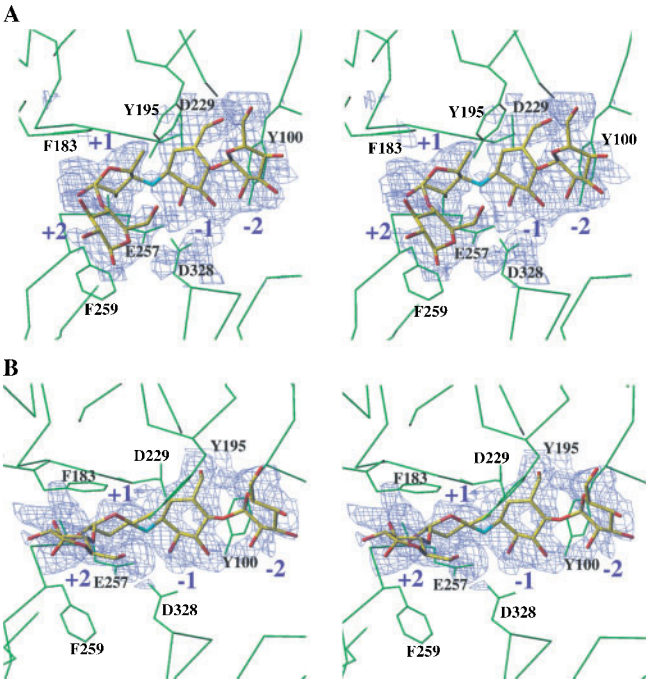

Fig. 3. **Stereoviews of pseudotetrasaccharide bound to molecules 1 (A) and 2 (B) of the wild type with omit $|F_o - F_c|$ electron density maps at the 1 σ level.** Active sites of molecules 1 and 2 of wild-type CGTase are shown with amino acid residues in contact with acarbose.

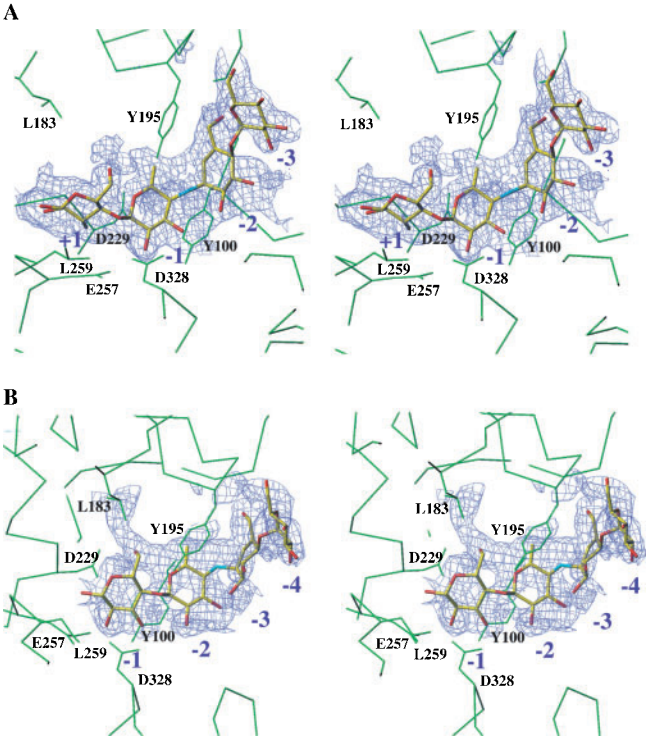

Fig. 4. **Stereoviews of pseudotetrasaccharide bound to molecules 1 (A) and 2 (B) of the F183L/F259L mutant with omit $|F_o - F_c|$ electron density maps at the 2 σ level.** Active site of molecules 1 and 2 of the F183L/F259L mutant are shown with amino acid residues in contact with acarbose.

dues at subsites –1 and +1 on molecule 1 but only with the D-glucose residue at subsite –1 on molecule 2 (not shown). In addition, molecule 1 of the F183L/F259L mutant indicated a linear-like mode of binding at subsite +1 because the stacking interaction between the sugar ring and Phe259 at subsite +2 was lost (Fig. 4A).

Because carbohydrate/aromatic stacking interaction was absent at subsite +2, the cleavage site of 3KB-G5-CNP was confined to bond 4, which corresponded to one of the two cleavage sites of the wild-type. That is, the shifts of the bond cleavage sites of 3KB-G5-CNP corresponded to the altered binding mode of GlcAcvGlc on the F183L/F259L mutant (Table 6).

On both molecules of the F183L/F259L mutant, significant conformational changes arose in the glycosidic linkage of the D-glucose residue of GlcAcvGlc at subsite +1 or –1 as compared with the equivalent sugar residues of GlcAcvGlc on wild-type molecules 1 and 2. These conformational changes were attributed to changes in the ψ [C1-O4′ (N4′)-C4′-C5′] torsion angles of residues located at subsites –1 to +1 of molecule 1 (–105.02° to –153.08°) and subsites –2 to –1 of molecule 2 (–98.19° to –132.86°) (Table 3B). The alteration in the torsion angle (ψ) on molecule 1 was larger than that on molecule 2. Thus, the pyranose ring of GlcAcvGlc was slightly more distant from the aromatic ring of Tyr100 at subsite –1 of molecule 1, and the pyranose ring of GlcAcvGlc was rather perpendicular to the aromatic side chain of Tyr100 at subsite –1 of molecule 2 compared with that of the wild-type (Fig. 4).

As shown in the omit $|F_o - F_c|$ electron density map of each molecule of the mutant Y100L-acarbose complex, the binding modes of acarbose on molecules 1 and 2 are quite different from those of the wild-type and the F183L/F259L mutant (Fig. 5). The glycosidic linkage of acarbose between the cyclitol ring and 4-amino-4, 6-dideoxy-D-glucose bound to molecule 1 was located far from Glu257 and moved from the active center towards the side chain of Tyr195. On molecule 2, the acarbose molecule shifted towards the non-reducing end compared with that on molecule 1. The glycosidic linkage between D-glucose and the next D-glucose residue was located far from Glu257 and also moved from the active center toward the side chain of Tyr195, as on molecule 1 of this mutant. In addition, acarbose is arc-shaped, because it is released from the restriction imposed by the side chains of both Phe183 and Phe259.

Electron density maps alone could not strictly identify whether GlcAcvGlc or acarbose was present in crystals of the Y100L-inhibitor complex. However, TLC analysis of the reaction products and kinetic data suggest that acarbose is present in the complex (Fig. 2 and Table 4, respectively). Moreover, the high IC_{50} value for acarbose of the Y100L mutant is reasonable considering that the acarbose binding feature is located far from the active site of this enzyme, and because changes in the IC_{50} correlate with changes in the affinity of acarbose for the enzyme (*13*).

When the carbohydrate/aromatic stacking interaction with Tyr100 at subsite –1 was absent, the number of hydrogen bonds between acarbose and the amino acid residues in the active site of molecules 1 and 2 significantly decreased (not shown). The D-glucose residues at

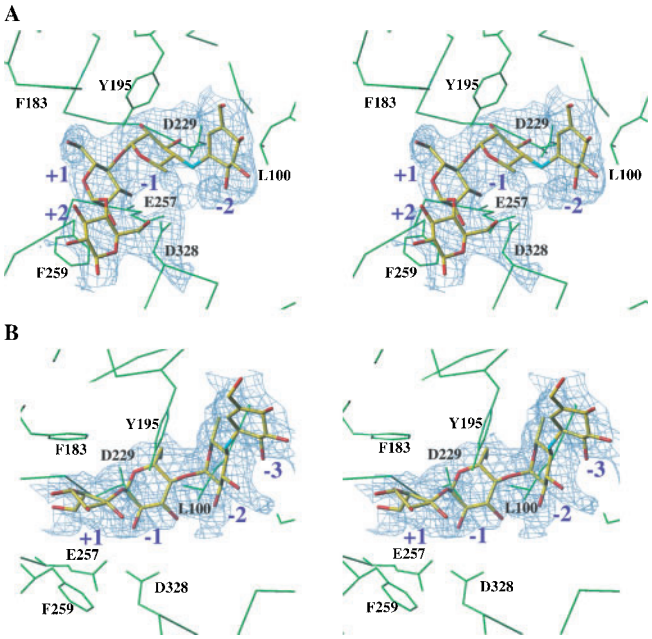

Fig. 5. **Stereoviews of acarbose bound to molecules 1 (A) and 2 (B) of the Y100L mutant with omit $|F_o - F_c|$ electron density maps at the 2 σ level.** Active sites of molecules 1 and 2 of the Y100L mutant are shown with amino acid residues in contact with acarbose.

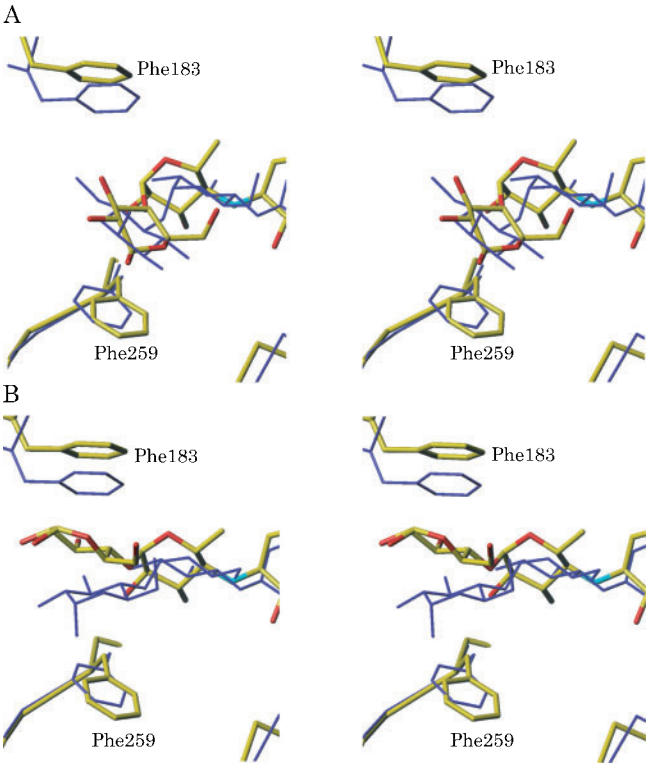

Fig. 6. **Stereoviews of structures of two pseudotetrasaccharide molecules bound at subsites +1 and +2 on molecules 1 (A) and 2 (B) of wild-type CGTase shown in thick lines.** For reference, structures of CGTase complexed with γ-CD (A) and maltononaose (B) reported by Uitdehaag *et al.* (*18*, *19*) are superimposed in thin blue lines.

subsites +1 and +2 on molecule 1 and at subsite +1 on molecule 2 of the Y100L mutant deviated from the stacking interaction with both Phe183 and Phe259. Consequently, the acarbose molecule vacated the active center and shifted to the side chain of Tyr195.

DISCUSSION

Phe259 Is Indirectly Involved in Substrate Binding at Subsites –1 and +1 through Stacking Interaction with the Sugar Ring at Subsite +2—The precise roles of Phe183 and Phe259 have been investigated by mutational analyses of the hydrophobic amino acid residues at subsite +2 of CGTase from *B. circulans* strain 251 (*38*). These two residues play distinct roles in transglycosylation, as observed in the cyclization reaction of CGTase from *B. circulans* strain 251 (*39*). In other words, Phe183 is involved in the initial binding of the acceptor maltose, while Phe259 is specifically important for cyclodextrin binding and is required for interaction that results in catalysis during disproportionation and cyclization. These results agree with our previous mutational data showing that Phe183 affects acceptor binding during transglycosylation. However, the effects of Phe259 on donor substrate binding during disproportionation and coupling have remained controversial.

The X-ray structure of the acarbose-F183L/F259L complex indicated that the binding modes of GlcAcvGlc shifted in the direction of the non-reducing end, corresponding to the shifts in the binding modes of 3KB-G5-CNP (Fig. 4 and Table 6). These data suggest that the large IC_{50} value for acarbose of the F183L/F259L mutant results from the location of the inhibitory acarviosine moiety far from the catalytic residues of this mutant, and from the apparently low affinity of the mutant for acarbose (Figs. 1 and 4).

With the shift of the binding modes of GlcAcvGlc, the ψ torsion angles of glycosidic linkages significantly change at subsites –1 to +1 of molecule 1 and at subsites –2 to –1 of molecule 2 (Table 3B). As a result, the sugar ring of GlcAcvGlc cannot normally bind at subsites –1 to +1 of each molecule on the F183L/F259L mutant: the sugar ring at subsite –1 of molecule 1 is a little far from Tyr100, and the sugar ring at subsite –1 of molecule 2 is perpendicular to the phenyl ring of Tyr100. We suggest that these observations are related to the absence of the carbohydrate/aromatic stacking interaction brought about by replacing Phe259 with leucine at subsite +2. Phe259 is directly involved in two binding modes (Fig. 6), and the K_m value of the F259L mutant for donor 3KB-G5-CNP tripled, while the k_{cat} decreased to 12% of the wild-type value. In contrast the K_m value of the F183L mutant was decreased by half, and the k_{cat} increased to 150% of the wild-type value (Table 4).

This notion is further supported by the fact that 1-deoxynojirimycin, a pseudo-monosaccharide that is a potent inhibitor of glucoamylase (*40*), is not stacked by Tyr100 at subsite –1 of CGTase from alkalophilic *Bacillus* sp. 1011 (*41*). This indicates that the binding of a pyranose ring at the catalytic subsite –1 requires the support of cooperative carbohydrate/aromatic interaction

and hydrogen-bonding contacts with the adjacent amino acid residues. We analyzed the role of Phe283, which is an essentially conserved aromatic residue among CGTases (*13*). The X-ray structures of the F283L mutant and its acarbose complex indicate that Phe259 is involved in stabilizing the structures at subsites +1 to +3 through hydrophobic interaction with Phe283, which is located under Phe259 and indirectly affects the orientation of the side chain of Glu257 (Kanai *et al*., unpublished). These results may be explained by the high K_m, which represents an alteration of the ground state binding, and the low k_{cat}/K_m value of the F259L mutant in the disproportionation reaction of 3KB-G5-CNP (Table 4).

All of these observations imply that Phe259 cooperates with Tyr100 in substrate binding at subsites –1 to +1 by controlling the conformation of the sugar residues at subsites –1 to +1 through the carbohydrate/aromatic stacking interaction at subsite +2.

Tyr100 Is of Critical Importance for Substrate Binding in the Active Site of CGTase—Replacing Tyr100 with leucine remarkably increased the IC_{50} for acarbose and completely diminished the CGTase activities without structurally changing the active site (Tables 4 and 5; Fig. 5). The three-dimensional structure of the wild-type in the complex with acarbose has shown that Tyr100 stacks the cyclitol ring of GlcAcvGlc at subsite –1 but does not form hydrogen bonds with cyclitol, which is in hydrogen-bond contacts with Glu257, Asp229, Asp328, His327, and Arg375, as it is in other family 13 enzymes complexed with acarbose (*32–36*). Furthermore, multiple contacts support the binding of sugar residues of acarbose at other subsites of the wild-type. Nevertheless, the sugar residues of acarbose bound in the stackless mutant Y100L had lost almost all hydrogen-bond contacts, and the glycosidic linkage of acarbose at subsites –1 to +1 of each molecule was located far from Glu257 because it had moved towards the side chain of Tyr195.

On the other hand, the Y100F mutant presumably retains the carbohydrate/aromatic stacking interaction with acarbose at subsite –1, since its K_m for 3KB-G5-CNP was similar with that of the wild-type (Table 4). In contrast, the k_{cat} for 3KB-G5-CNP significantly decreased (to 7% of the wild-type value). The hydroxyl group of Tyr100 forms a hydrogen bond with the side chain of His327 (molecules 1 and 2) and also contacts Arg227 (water-mediated on molecule 1), Asp135 (water-mediated on molecule 2), and Glu257 (water-mediated on molecule 1), which constitutes the catalytic subsite –1 of the wild-type enzyme complexed with acarbose. Therefore, the mutation of Tyr100 to phenylalanine may affect the proper conformations of side chains of these residues, which are critically important for the catalytic activity of CGTase (*42*). Observations of the alkalophilic *Bacillus* sp. I-5 CGTase have shown that the Y100S mutant has no detectable starch-degrading or β-CD forming activities, and that the mutation significantly affects coupling activity (*43*).

The stacking interaction between Tyr100 and the sugar ring is of particular importance for the substrate binding of CGTase, even though many interactions proceed through hydrogen bonds between the sugar residues of acarbose and subsite –1. Many highly refined X-ray structures of ligand forms of carbohydrate-binding protein have indicated that several hydrogen bonds are the key factors related to the specificity and affinity of protein/carbohydrate interaction (*44*, *45*). However, the absence of a stacking interaction with Leu100, Leu183, and Leu259 might affect the binding mode and alter hydrogen-bond contacts between acarbose and mutant enzymes.

The role of the carbohydrate/aromatic stacking interaction with Tyr100, Phe259, and Phe183 seems to fix the pyranose ring of substrates in appropriate positions and to determine their orientation, thus stabilizing interactions between sugar substrates and subsites. On the other hand, hydrogen bonds play a major role in transition state stabilization, but their high flexibility might prevent them from playing a key role in positioning. These characteristic differences between stacking interactions and hydrogen-bonding contacts could explain our present results.

The significant differences between the mutational analyses of Y100L and Y83L (equivalent to Tyr100) mutants from Sfamy (*24*) seem ascribable to aromatic residues such as Phe183 and Phe259 at subsite +2, which are suitable for the successive and varied reactions catalyzed by CGTases. Therefore, these residues might constitute a key factor with which to determine functional differences between CGTases and α-amylases.

We thank Drs. A. Mullen and K. Hornberg for supplying acarbose, Dr. H. Takahasi for proving *E. coli* strain ME8417, and Dr. S. Sakai for providing Amylose (DP = 17). We also thank N. Foster for critical reading of the manuscript. This work was supported in part by Grants-in-Aid from the Ministry of Education, Science, Sports, Culture and Technology Japan, and by a Grant from the Rice Genome Project PR-2212, MAFF, Japan.

REFFERNCES

1. Binder, F., Huber, O., and Böck, A. (1986) Cyclodextrin glycosyltransferase from *Klebsiella pneumoniae* M5a1. Cloning, nucleotide sequence and expression. *Gene* **47**, 269–277
2. Kimura, K., Kataoka, S., Ishii, Y., Takano, T., and Yamane, K. (1987) Nucleotide sequence of the β-cyclodextrin glucanotransferase gene of alkalophilic *Bacillus* sp. strain 1011 and similarity of its amino acid sequence to those of α-amylases. *J. Bacteriol.* **169**, 4399–4402
3. Katsuragi, N., Takizawa, N., and Murooka, Y. (1987) Entire nucleotide sequence of the pullulanase gene of *Klebsiella aerogenes* W70. *J. Bacteriol.* **169**, 2301–2306
4. Matsuura, Y., Kusunoki, M., Harada, W., and Kakudo, M. (1984) Structure and possible catalytic residues of Taka-amylase A. *J. Biochem. (Tokyo).* **95**, 697–702
5. Qian, M., Haser, R., and Payan, F. (1993) Structure and molecular model refinement of pig pancreatic α-amylase at 2.1 Å resolution. *J. Mol. Biol.* **231**, 785–799
6. Hofman, B.E., Bender, H., and Schulz, G.E. (1989) Three-dimensional structure of cyclodextrin glycosyltransferase from *Bacillus circulans* at 3.4 Å resolution. *J. Mol. Biol.* **209**, 793–800
7. Boel, E., Brzozowski, A.M., Derewenda, Z., Dodson, G.G., Jensen, V.J., Peterson, S.B., Swift, H., Thim, L., and Woldike, H.F. (1990) Calcium binding in α-amylases: an X-ray diffraction study at 2.1-Å resolution of two enzymes from *Aspergillus*. *Biochemistry* **29**, 6244–6249
8. Klein, C. and Schulz, G.E. (1991) Structure of cyclodextrin glycosyltransferase refined at 2.0 Å resolution. *J. Mol. Biol.* **217**, 737–750

9. Kubota, M., Matsuura, Y., Sakai, S., and Katsube, Y. (1991) Molecular structure of *B. stearothermophilus* cyclodextrin glucanotransferase and analysis of substrate binding site. *Denpun Kagaku* **38**, 141–146
10. Nakamura, A., Haga, K., Ogawa, S., Kuwano, K., Kimura, K., and Yamane, K. (1992) Functional relationships between cyclodextrin glucanotransferase from an alkalophilic *Bacillus* and α-amylases. Site-directed mutagenesis of the conserved two Asp and one Glu residues. *FEBS Lett.* **296**, 37–40
11. Nakamura, A., Haga, K., and Yamane, K. (1993) Three histidine residues in the active center of cyclodextrin glucanotransferase from alkalophilic *Bacillus* sp. 1011: effects of the replacement on pH dependence and transition-state stabilization. *Biochemistry* **32**, 6624–6631
12. Nakamura, A., Haga, K., and Yamane, K. (1994) The transglycosylation reaction of cyclodextrin glucanotransferase is operated by a Ping-Pong mechanism. *FEBS Lett.* **337**, 66–70
13. Nakamura, A., Haga, K., and Yamane, K. (1994) Four aromatic residues in the active center of cyclodextrin glucanotransferase from alkalophilic *Bacillus* sp. 1011: effects of replacements on substrate binding and cyclization characteristics. *Biochemistry* **33**, 9929–9936
14. Haga, K., Harata, K., Nakamura, A., and Yamane, K. (1994) Crystallization and preliminary X-ray studies of cyclodextrin glucanotransferase from alkalophilic *Bacillus* sp. 1011. *J. Mol. Biol.* **237**, 163–164
15. Harata, K., Haga, K., Nakamura, A., Aoyagi, M., and Yamane, K. (1996) X-ray structure of cyclodextrin glucanotransferase from alkalophilic *Bacillus* sp. 1011. Comparison of two independent molecules at 1.8 Å resolution. *Acta Cryst.* **D52**, 1136–1145
16. Lawson, C.L., van Montfort, R., Strokopytov, B., Rozeboom, H.J., K.H., de Vries, G., Penninga, D., Dijkhuizen, L., and Dijkstra, B.W. (1994) Nucleotide sequence and X-ray structure of cyclodextrin glycosyltransferase from *Bacillus circulans* strain 251 in a maltose-dependent crystal form. *J. Mol. Biol.* **236**, 590–600
17. Knegtel, R.M.A., Wind, R.D., Rozeboom, H.J., Kalk, K.H., Buitelaar, R.M., Dijkhuizen, L., and Dijkstra, B.W. (1996) Crystal structure at 2.3 Å resolution and revised nucleotide sequence of the thermostable cyclodextrin glycosyltransferase from *Thermoanaerobacterium thermosulfurigenes* EM1. *J. Mol. Biol.* **256**, 611–622
18. Strokopytov, B., Knegtel, R.M.A., Penninga, D., Rozeboom, H.J., Kalk, K.H., Dijkhuizen, L., and Dijkstra, B.W. (1996) Structure of cyclodextrin glycosyltransferase complexed with a maltononaose inhibitor at 2.6 Å resolution. Implications for product specificity. *Biochemistry* **35**, 4241–4249
19. Uitdehaag, J.C.M., Kalk, K.H., van der Veen, B.A., Dijkhuizen, L., and Dijkstra, B.W. (1999) The cyclization mechanism of cyclodextrin glycosyltransferase (CGTase) as revealed by a γ-cyclodextrin-CGTase complex at 1.8-Å resolution. *J. Biol. Chem.* **274**, 34868–34876
20. Uitdehaag, J.C.M., Mosi. R., Kalk, K.H., van der Veen, B.A., Dijkhuizen, L., and Dijkstra, B.W. (1999) X-ray structures along the reaction pathway of cyclodextrin glycosyltransferase elucidate catalysis in the α-amylase family. *Nat. Struct. Biol.* **6**, 432–436
21. Uitdehaag, J.C.M., van Alebeek, G.J.W.M., van der Veen, B.A., Dijkhuizen, L., and Dijkstra, B.W. (2000) Structures of maltohexaose and maltoheptaose bound at the donor sites of cyclodextrin glycosyltransferase give insight into the mechanisms of transglycosylation activity and cyclodextrin size specificity. *Biochemistry* **39**, 7772–7780
22. Parsiegla, G., Schmidt, A.K., and Schulz, G.E. (1998) Substrate binding to a cyclodextrin glycosyltransferase and mutations increasing the γ-cyclodextrin production. *Eur. J. Biochem.* **255**, 710–717
23. Schmidt, A.K., Cottaz, S., Driguez, H., and Schulz, G.E. (1998) Structure of cyclodextrin glycosyltransferase complexed with a derivative of its main product β-cyclodextrin. *Biochemistry* **37**, 5909–5915
24. Matsui, I., Yoneda, S., Ishikawa, K., Miyairi, S., Fukui, S., Umeyama, H., and Honda, K. (1994) Roles of the aromatic residues conserved in the active center of *Saccharomycopsis* α-amylase for transglycosylation and hydrolysis activity. *Biochemistry* **33**, 451–458
25. Kunkel, T.A., Roberts, J.D., and Zakour, R.A. (1987) Rapid and efficient site-specific mutagenesis without phenotypic selection. *Methods Enzymol.* **154**, 367–382
26. Sanger, F., Nicklen, S., and Coulson, A.R. (1977) DNA sequencing with chain-termination inhibitors. *Proc. Natl. Acad. Sci. USA* **74**, 5463–5467
27. Chan, S.J., Weiss, J., Konrad, M., White, T., Bahl, C., Yu, S.D., Marks, D., and Steiner, D.F. (1981) Biosynthesis and periplasmic segregation of human proinsulin in *Escherichia coli*. *Proc. Natl. Acad. Sci. USA* **78**, 5401–5405
28. Fuwa, H. (1954) A new method for microdetermination of amylase activity by use of amylose as a substrate. *J. Biochem. (Tokyo)* **41**, 583–603
29. Brünger, A.T., Kuriyan, J., and Karplus, M. (1987) Crystallographic *R* factor refinement by molecular dynamics. *Science* **235**, 458–460
30. Laskowski, A.R., MacArthur, M.W., Moss, D.S., and Thornton, J.M. (1993) PROCHECK: a program to check the stereochemical quality of protein structures. *J. Appl. Crystallogr.* **26**, 283–291
31. Przylas, I., Terada, Y., Fujii, K., Takaha, T., Saenger, W., and Strater, N. (2000) X-ray structure of acarbose bound to amylomaltase from *Thermus aquaticus*. Implications for the synthesis of large cyclic glucans. *Eur. J. Biochem.* **267**, 6903–6913
32. Qian, M., Haser, R., Buisson, G., Duee, E., and Payan, F. (1994) The active center of a mammalian α-amylase. Structure of the complex of a pancreatic α-amylase with a carbohydrate inhibitor refined to 2.2 Å resolution. *Biochemistry* **33**, 6284–6294
33. Gilles, C., Astier, J.-P., Marchis-Mouren, G., Cambillau, C., and Payan, F. (1996) Crystal structure of pig pancreatic α-amylase isoenzyme II, in complex with the carbohydrate inhibitor acarbose. *Eur. J. Biochem.* **238**, 561–569
34. Brzozowski, A.M. and Davies, G.J. (1997) Structure of the *Aspergillus oryzae* α-amylase complexed with the inhibitor acarbose at 2.0 Å resolution. *Biochemistry* **36**, 10837–10845
35. Kadziola, A., Søgaard, M., Svensson, B., and Haser, R. (1998) Molecular structure of a barley α-amylase-inhibitor complex: implications for starch binding and catalysis. *J. Mol. Biol.* **278**, 205–217
36. Mosi, R., Sham, H., Uitdehaag, J.C.M., Ruiterkamp, R., Dijkstra, B.W., and Withers, S.G. (1998) Reassessment of acarbose as a transition state analogue inhibitor of cyclodextrin glycosyltransferase. *Biochemistry* **37**, 17192–17198
37. Kim, M.J., Lee, H.S., Cho, J.S., Kim, T.J., Moon, T.W., Oh, S.T., Kim, J.W., Oh, B.H., and Park, K.H. (2002) Preparation and characterization of α-D-glucopyranosyl-α-acarviosinyl-D-glucopyranose, a novel inhibitor specific for maltose-producing amylase. *Biochemistry* **41**, 9099–9108
38. van der Veen, B.A., Leemhuis, H., Kralj, S., Uitdehaag, J.C.M., Dijkstra, B.W., and Dijkhuizen, L. (2001) Hydrophobic amino acid residues in the acceptor binding site are main determinants for reaction mechanism and specificity of cyclodextrin glycosyltransferase. *J. Biol. Chem.* **276**, 44557–44562
39. Uitdehaag, J.C.M., van der Veen, B.A., Dijkhuizen, L. Elber, R., and Dijkstra, B.W. (2001) Enzymatic circularization of a maltooctaose linear chain studied by stochastic reaction path calculations on cyclodextrin glycosyltransferase. *Proteins* **43**, 327–335
40. Truscheit, E., Frommer, W., Junge, B., Müller, L., Schmidt, D.D., and Wingender, W. (1981) Chemistry and biochemistry of microbial α-glucosidase inhibitors. *Angew. Chem. Int. Ed. Engl.* **20**, 744–761
41. Kanai, R., Haga, K., Yamane, K., and Harata, K. (2001) Crystal structure of cyclodextrin glucanotransferase from alkalophilic *Bacillus* sp. 1011 complexed with 1-deoxynojirimycin at 2.0 Å resolution. *J. Biochem. (Tokyo)* **129**, 593–598

42. Leemhuis, H., Rozeboom, H.J., and Dijkstra, B.W., and Dijkhuizen, L. (2003) The fully conserved Asp residue in conserved sequence region I of the α-amylase family is crucial for the catalytic site architecture and activity. *FEBS Lett.* **541**, 47–51
43. Kim, Y.H., Bae, K.H., Kim, T.J., Park, K.H., Lee, H.S., and Byun, (1997) Effect on product specificity of cyclodextrin glycosyltransferase by site-directed mutagenesis. *Biochem. Mol. Biol. Int.* **41**, 227–234
44. Sharon, N. (1993) Lectin-carbohydrate complexes of plants and animals: an atomic view. *Trends Biochem. Sci.* **18**, 221–226
45. Spurlino, J.C., Lu, G-Y., and Quiocho, F.A. (1991) The 2.3-Å resolution structure of the maltose- or maltodextrin-binding protein, a primary receptor of bacterial active transport and chemotaxis. *J. Biol. Chem.* **266**, 5202–5219
46. Rogers, J.C. and Milliman, C. (1983) Isolation and sequence analysis of a barley α-amylase cDNA clone. *J. Biol. Chem.* **258**, 8169–8174
47. Nakao, M., Nakayama, T., Harada, M., Kakudo, A., Ikemoto, H., Kobayashi, S., and Shibano, Y. (1994) Purification and characterization of a *Bacillus* sp. SAM1606 thermostable α-glucosidase with transglucosylation activity. *Appl. Microbiol. Biotechnol.* **41**, 337–343